Encapsulation of cadmium telluride nanocrystals within single walled carbon nanotubes

Kuganathan, N. & Chroneos, A.

Encapsulation of Cadmium Telluride Nanocrystals within Single Walled Carbon Nanotubes

Navaratnarajah Kuganathan[2,a)] and Alexander Chroneos[1,2,b)]

[1]Department of Materials, Imperial College London, London, SW7 2AZ, United Kingdom

[2]Faculty of Engineering, Environment and Computing, Coventry University, Priory Street, Coventry CV1 5FB, United Kingdom

_____

Abstract

The encapsulation of crystal structures of cadmium telluride within small diameter single walled nanotubes (SWNTs) are studied using density functional theory with a dispersion correction (DFT+D). Four different suitable pseudo one-dimensional (1-d) CdTe crystals were considered and their energies were compared. The isolated **4:2** crystal (derived from the hexagonal CdTe bulk) was calculated to be the most thermodynamically stable of the four structures. Calculations were performed on the **4:2** crystal inserted into three different SWNTs, (8, 8), (9, 9), and (10, 10), in order to investigate energy of formation of the CdTe@SWNT composites. The calculated encapsulation energies show that the interaction between nanotubes and the CdTe crystals is noncovalent. Since the energy difference of the "free" **4:2** and **3:3** structures is small(0.07 eV/CdTe), we carried out calculations on **3:3** CdTe structure encapsulated in to two different SWNTs, (9, 9) and (10,10). The calculated encapsulation energies are exoergic suggesting that this polymporph may also be found experimentally. The other two structures are also encapsulated and their results are discussed though they can be found within SWNTs at high temperatures. The present study proposes that both **4:2** and **3:3** CdTe structures can be observed in the microscopic experiments and further experimental verification is required.

[1]Corresponding authors, e-mails: a) ad0636@coventry.ac.uk b) alexander.chroneos@imperial.ac.uk

1. Introduction

Single-walled carbon nanotubes (SWNTs)[1,2] are promising candidate materials to synthesise low-dimensional materials owing to their hollow cavities which allow bulk materials to form novel one dimensional crystals. In many cases the encapsulation of bulk materials introduces a change in their coordination leading to different physical and chemical properties of both guest and host[3]. Low-dimensional materials formed within SWNTs have attracted considerable attention due their applications in nanoelectronics and energy storage devices. Therefore, the encapsulation or filling of SWNTs with a variety of novel materials has been achieved by several experimental methods and their reduced dimensional structures have been well characterised by advanced microscopic techniques[4–6].

Cadmium telluride (CdTe) is an important semiconductor material in optoelectronics and solar cells[7]. There is a growing interest to make one dimensional CdTe structures such as nanotubes, nanowires, nanorods and nanocables in order to optimise their electronic, optical, mechanical and catalytic properties in areas such as electronics, energy storage and nanodevices. Chong *et al.*[8] reported a novel electrochemical approach to synthesis CdTe/SWNT hybrid nanostructures to tune the electrical and optoelectrical properties of CdTe. Haijun *et al.*[9] synthesised long CdTe nanotubes of different diameters using cadmium thiolate polymer. There is a limited experimental study on CdTe nanostructure composites and no report available in the literature on 1-d CdTe crystals encapsulated within SWNTS.

SWNTs have been considered as ideal containers to form various foreign species including one dimensional inorganic nanocrystals[3, 10-12]. In the past decade, a variety of metal halides and metal chalcogenides have been encapsulated within SWNTs experimentally[4–6, 13–15]. Sloan *et al.*[13] reported the filling of SWNTs with KI and observed an 1-d 2×2 KI nanocrystals along the tube axis. This 1-d crystal exhibits a 4:4 coordination without showing an overall change in the structure but a systematic reduction in the coordination from its bulk (i.e. 6:6). A novel 1-d structure of mercury telluride with 3:3 coordination grown inside SWNTs was reported by Carter *et al.*[14] In this novel structure both structure and coordination totally are different from its bulk zinc blende HgTe crystal which exhibits 4:4 coordination. Recently, encapsulation of CdSe within SWNT cavities has been experimentally characterised for the future application in nano-biotechnology[16]. Three different types of 1-d PbTe nanocrystals have been recently found inside narrow SWNTs using high-resolution transmission electron microscopy (HRTEM) and their size of the structures were correlated with SWNTs having different diameters[17].

Computational modelling techniques are powerful tools to validate the experimentally determined 1-d crystal structures or molecules confined into SWNTs and predict the electronic properties of the composites. There are many theoretical studies available on the molecular structures

encapsulated within SWNTs[18-28]. However, only few theoretical reports are available to model experimentally observed 1-d crystals such as KI[29], HgTe[30], CuI[31], PbI2[32], Sb$_2$Se$_3$[33], SnSe[34], AgI[35], CdSe[16] and PbTe[17]). In some cases, HRTEM images of 1-d crystals containing lighter atoms are challenging to demonstrate their structures because of their lower resolution. In such cases model structures should be proposed to generate images for comparison with experiment. In a previous study[31], we proposed model structures for CuI nanocrystals that can be found inside SWNTs. Recently, we proposed possible model structures for CdSe and confirmed that one of the proposed structures agreed well with the experiment[16]. In some cases, calculated model structures are highly ordered compared to those found in HRTEM experiments. Fu *et al.*[36,37] recently studied the formation of Sulfur chain inside SWNTs both experimentally and computationally. Computed structure from their study shows that the disordered structure of the Sulphur chain is more stable inside SWNT compared to the ordered structures (linear and zig-zag).

In this present study, we propose possible 1-d CdTe crystal structures that may be found experimentally within different diameters of SWNTS. Here the simulations are based on the previous experimental 1-d structure of HgTe found inside SWNT and possible model structures retrieved from different CdTe bulk structures. The experimental structure of HgTe was considered as a starting configuration for CdTe because as both Hg and Cd are in the same group in the periodic table. Here we calculate encapsulation energies to predict the thermodynamical stability of the CdTe crystals inside SWTs, charge transfer between the CdTe nanocrystals and SWNTs and electronic structures for the most stable SWNT/CdTe composites.

2. Computational methods

DFT calculations were performed on 1-d CdTe crystals and nanowires encapsulated within SWNTs to determine the electronic structure and the nature of the interaction between the CdTe and the nanotubes. The VASP code[38,39], which solves the standard Kohn-Sham (KS) equations using plane wave basis sets was employed in all calculations. For the exchange correlation term, we used the Generalised Gradient Approximation (GGA) parameterised by the Perdew-Burke-Ernzerhof (PBE)[40] functional. The choice of this functional is based on the previous simulations which showed excellent agreement with experimental results[16, 23-27]. The standard projected augmented wave (PAW) potentials[41] and a plane-wave basis set with a cut off value of 500 eV were employed for all atoms. The valence electronic configurations for Cd, Te and C were $4d^{10}5s^2$, $5s^25p^4$ and $2s^22p^2$ respectively. Structure optimizations were performed using a conjugate gradient algorithm[42] and the forces on the atoms were obtained from the Hellman-Feynman theorem including Pulay corrections. In all optimised structures, forces on the atoms were smaller than 0.001 eV/Å and the stress tensor was less than 0.02 GPa. In all calculations, both SWNTs and CdTe nanocrystals were treated as infinite structures along the tube axis using periodic boundary

conditions. In the other two directions, a separation of 25 Å was applied to make sure that the nanotubes do not interact with their periodic images. A detail information regarding the number of atoms involved in each composites and the Monkhorst pack k points[43] used are given in the ESI. The inclusion of van der Waals (vdW) interactions is particularly important for the encapsulation of 1-d crystals into the SWNTs . Here, dispersion has been included by using the pair-wise force field as implemented by Grimme *et al.*[44] (DFT-D3) in VASP. In our recent work, the difference in the binding energies with and without dispersion correction was observed[45].

The encapsulation energy of CdTe crystal found in a SWNT is defined by the difference in the total energy of the CdTe@SWNT composite and the total energies calculated for an isolated CdTe crystal and an isolated SWNT.

$$E_{encaps} = E_{CdTe@SWNT} - E_{CdTe} - E_{SWNT} \tag{1}$$

where $E_{CdTe@SWNT}$ is the total energy of CdTe encapsulated within a SWNT ; E_{CdTe} and E_{SWNT} are the total energies of isolated CdTe and SWNT repectively.

3. Results and Discussion

3.1. Calculation on bulk CdTe

The quality of the pseudopotentials and basis sets for Cd and Te was tested by performing calculations on bulk zinc blende CdTe (space group $F\bar{4}3m$) as shown in Figure 1a. Single point calculations were performed on bulk CdTe structure to obtain the equilibrium lattice constants and bulk modulus (see Table 1). The bulk volume was allowed to vary within ±5 % of the equilibrium volume. Figure 1b shows the cohesive curve plotted by fitting values of the calculated energy in the Murnaghan equation of state[46]. The calculated equilibrium lattice constant (6.54 Å) and bulk modulus (39.1 GPa) derived from the Murnaghan fit were in good agreement with the experimental[47-50] and the other theoretical values[51-53] showing the validity of the pseudopotentials and basis sets. The DOS calculated for bulk CdTe is shown in Figure 1c. The calculation indicates that CdTe bulk is a semiconductor with a band gap of 1.60 eV which is in good agreement with the experimental values of 1.44 eV and 1.60 eV reported by Kittel *et al*[54]. and Strehlow *et al.*[55] respectively.

3.2. One dimensional crystals of CdTe

Here, we propose four different starting structures for 1-d CdTe crystals that can be observed inside the SWNTs (see Figure 2). All four structures were treated as infinite crystals and optimized with periodic boundary conditions. The initial and corresponding optimized structures are depicted in Figure 2.

The first starting structure (**4:2**) is derived from the hexagonal CdTe bulk structure. The selection of this structure is based on our previous modeling of CdSe crystal encapsulated within SWNTs[16]. In this initial structure, Cd and Te form four and two coordination respectively. Relaxation of the **4:2** crystals led to a distorted structure in which both Cd and Te form three-fold coordination and this structure is calculated to be the lowest energy structure (refer to Table 2). In the case of CdSe, it was found that **4:2** structure is the second most stable structure only higher energy by 0.07 eV than that of **3:3** structure (more detail of this structure is explained in the next section). The Cd-Te bond distances are slightly longer than that of Cd-Se due to the smaller atomic radius of Se than Te.

The second proposed structure (**3:3**) is a novel structure experimentally found for HgTe inside SWNTs[14]. As both Hg and Cd are in the same group of the periodic table, it seemed reasonable to propose this **3:3** HgTe structure for CdTe. In our previous modelling, we proposed this structure as a starting structure for 1-d CuI and CdSe nanocrystals. The **3:3** Cd forms a trigonal planar structure (CdTe$_3$) with adjacent Te atoms and Te forming a trigonal pyramidal environment (TeCd$_3$) with three nearest neighbor Cd atoms. The calculated Cd-Te bonds, Cd-Te-Cd and Te-Cd-Te bond angles are very close to the values observed for HgTe crystals observed inside SWNTs retaining its initial configuration. The calculation shows that the **3:3** structure is the second most stable form of CdTe. The relaxed structure and energetics of **4:2** CdTe crystal indicate that its formation from **3:3** CdTe structure or vice versa is thermodynamically feasible.

The third starting structure is derived from the CdTe rock salt bulk structure with **4:4** coordination of atoms. This structure was previously considered to model experimentally observed KI crystal encapsulated within SWNTs by Sceats *et al.*[29] In previous work[16], we considered this structure as one of the staring starting structures to model HgTe and CdSe. The optimized structure of **4:4** CdTe gives a rhombohedral shape as observed for other one dimensional crystals (i.e. HgTe and CdSe). The distances of the Cd-Te bonds (2.92 -3.00 Å) were longer and bond angles larger than that found in the **3:3** or **4:2** structures. The initial structures of both the **4:4** and the **3:3** structures exhibit 2×2 cross-sections. In the **4:4** structure, four atoms (2Cd and 2Te) are at the corners of a square. But the four atoms are at the corners of a parallelogram in the **3:3** structure. Optimization of the **4:4** crystals did not lead to the lower energy **3:3** structure, presumably because the **4:4** structure is a local minimum.

The fourth starting structure is a chain structure derived from the cinnabar CdTe bulk structure in which both Cd and Te have two coordination (**2:2**). The optimized **2:2** structure within periodic boundary conditions gives a structure resembling the starting structure. In the optimized structure the Cd-Te bond distances are slightly shorter than the values calculated in the other

three relaxed structures and larger than the values found in the bulk cinnabar CdTe structure. The Te-Cd-Te and Cd-Te-Cd angles are found to be 178° and 89° in the optimized structure. In the bulk structure these values are 173° and 105° respectively.

Figure 3 shows the density of states plotted for gas phase 1-d CdTe crystals. There is an increase in the band-gap compared to that of bulk CdTe. This indicates that the formation of low dimensional CdTe crystals via encapsulation within SWNTs is an efficient engineering strategy to make semi-conducting devices.

3.3. Encapsulation of CdTe nanocrystals within SWNTs.

Three sizes of SWNTs were selected to encapsulate the CdTe nanocrystals. They are (8,8), (9,9) and (10,10) with diameters of 10.85 Å, 12.36 Å and 13.56 Å respectively. The selection of diameters is based on the one dimensional CdSe nanocrystals observed experimentally in a (9,9) tube[16]. As there are no experimental report available for the CdTe crystals, we considered two more SWNTs [(8,8) and (10,0)] with slightly different diameters.

3.3.1. 4:2 CdTe crystal encapsulated within SWNTs

First we encapsulated the most stable **4:2** CdTe nanocrystals in three different tubes and optimized the composites. Geometrical parameters, encapsulation energies and charge transfer calculated for **4:2** CdTe crystals encapsulated within three SWNTs are tabulated in Table 3. In addition, structural parameters calculated for the isolated CdTe crystal are also listed. The optimized structures of composites and corresponding charge density plots are shown in Figure 4. Analysis of calculated structural parameters indicates that as the diameter of SWNTs decreases, the CdTe crystal becomes compressed as evidenced by the cross-sectional view of the optimized structures (refer to Figure 4) and charge density plots. In the case of smaller (8,8) tube, distortion is more evident in the bond distances and bond angles compared to those calculated for the isolated gas phase 1-d CdTe crystals.

The calculated encapsulation energies indicate that in both (9,9) and (10,10) SWNTs, the formation of **4:2** CdTe is exoergic suggesting that they are thermodynamically stable. Endothermic encapsulation energy (+0.47 eV) is calculated for (8,8) SWNT as this tube has a smaller diameter and this is evidenced by the structural distortion. Bader charge analysis was carried out to calculate the charge transfer occurred between the tubes and CdTe nanocrystals. In all cases, a small amount of electrons has been transferred from CdTe crystals to the tubes. Larger charge transfer is observed for smaller tube as the encapsulated crystal is more closer to the tube walls.

3.3.2. 3:3 CdTe crystal encapsulated within SWNTs

Next we considered the encapsulation of the second most stable **3:3** CdTe structure. The optimized structures and charge density plots are shown in Figure 5. Table 4 reports the structural parameters, encapsulation energies and charge transfer. Energy minimization of CdTe encapsulated within (8,8) tube was not achieved due to the strong perturbation introduced on the composite during the optimization. Intermediate configuration was analyzed and the semi-relaxed structure is totally different from the initial structure. Therefore, we only report the values calculated for (9,9) and (10,10) tubes. Structural parameters indicate that **3:3** CdTe nanocrystals within smaller tube become distorted as evidenced by the shorter bond distances and larger bond angles compared to those calculated for the isolated 1-d **3:3** crystal. This is reflected in the encapsulation energy. The formation of **3:3** crystal within both tubes is exothermic. The lower encapsulation energy is observed for (9,9) tube as expected. In both cases, charge transfer is observed from CdTe crystals to tubes. A slightly larger amount of electrons is transferred in the case of (9,9) tube due to its smaller diameter.

3.3.3. 4:4 CdTe crystal encapsulated within SWNTs

Here we discuss structure and encapsulation nature of **4:4** CdTe crystal encapsulated in SWNTs. Structural parameters (refer to Table 5) indicate that crystal become compressed when it is encapsulated within the smaller tube. This is reflected in the Cd-Te bond length and angles. The **4:4** crystal enclosed within larger SWNTs have bond lengths and angles closer to the calculated gas phase values. There is no significant change in the structural parameters between the optimized CdTe structure in the isolated form and with the (10,10) tube indicating the small influence of the tube-wall interaction. In all three tubes, the encapsulation is exothermic. The CdTe crystal is stable even in the smaller (8,8) tube because of the smaller size of the crystal. Again the nature of encapsulation is non-covalent and a small amount of charge is transferred. The optimized structures and charge density plots are shown in Figure 6. The **4:4** structure is 0.46 eV/CdTe higher energy than the **4:2** structure, the formation of this complex is possible only at high temperatures.

3.3.4. 2:2 CdTe crystals encapsulated within SWNTs

Finally, we considered the encapsulation of **2:2** crystal. Shorter Cd-Te bond lengths and longer bond angles are observed for smaller tube as expected. Stronger encapsulation energies are observed for this crystal compared to the other three crystal structures though the **2:2** structure is the least stable structure to form. Therefore this structure is not formed at operating temperatures. The stronger encapsulation energy means the crystal has lesser distortion introduced by the tubes. Small charge transfer is observed due to the less number of atoms in the crystal interacting with nanotubes.

Figure 7 shows the relaxed structures together with the charge density plots. Table 6 reports the structural parameters, encapsulation energies and the amount of charge transfer occurred between the tubes and the crystals.

4. Conclusions

In conclusion, the encapsulation of the possible 1-d CdTe crystals inside was studied using DFT calculations. A CdTe crystal structure with a **4:2** initial coordination environment was found to be thermodynamically more stable than the other three motifs. The **3:3** structure is higher in energy by 0.07 eV compared to that of **4:2** structure. The first two stable (**4:2** and **3:3**) structures were first encapsulated within three different SWNTs. The encapsulation energies for the formation of these two CdTe crystals within the nanotubes are exoergic suggesting that they are stable inside SWNTs with the formation of non-covalent interaction. This is evidenced by the small amount of charge transferred from CdTe crystals to the tubes. The other two CdTe crystal structures **4:4** and **2:2**) were also inserted and their encapsulation energies calculated. Their encapsulation energies are exoergic too. However, their thermodynamical stabilities are high compared to those with the other two crystals, they would not be observed at operating temperatures. The current study provides two soundly based 1-d crystal models (**4:2** and **3:3**) for the experimentalists to use these models in their future experimental interpretation.

Supplementary data

Number of atoms considered to model pristine carbon nanotubes and composites of CdTe@SWNT is provided. Also number of Monkhorst k points used to optimise the composites is also provided.

References

1. D.S. Bethune, C.H. Kiang, M.S. de Vries, G. Gorman, R. Savoy, J. Vazquez, R. Beyers, Nature 363 (1993) 605.

2. S. Iijima, T. Ichihashi, Nature 363 (1993) 603.

3. J. Sloan, A.I. Kirkland, J.L. Hutchison, M.L.H. Green, Chemical Communications (2002) 1319.

4. C. Xu, J. Sloan, G. Brown, S. Bailey, V.C. Williams, S. Friedrichs, K.S. Coleman, E. Flahaut, J.L. Hutchison, R.E. Dunin-Borkowski, M.L.H. Green, Chemical Communications (2000) 2427.

5. A. Vasylenko, S. Marks, J.M. Wynn, P.V.C. Medeiros, Q.M. Ramasse, A.J. Morris, J. Sloan, D. Quigley, ACS Nano 12 (2018) 6023.

6. J. Sloan, S.J. Grosvenor, S. Friedrichs, A.I. Kirkland, J.L. Hutchison, M.L.H. Green, Angewandte Chemie International Edition 41 (2002) 1156.

7. T.L. Chu, S.S. Chu, Progress in Photovoltaics: Research and Applications 1 (1993) 31.

8. C.H. Chang, H. Jung, Y. Rheem, K.-H. Lee, D.-C. Lim, Y. Jeong, J.-H. Lim, N.V. Myung, Nanoscale 5 (2013) 1616.

9. H. Niu, M. Gao, Angewandte Chemie International Edition 45 (2006) 6462.

10. P.M.F.J. Costa, J. Sloan, T. Rutherford, M.L.H. Green, Chemistry of Materials 17 (2005) 6579.

11. L.-J. Li, A.N. Khlobystov, J.G. Wiltshire, G.A.D. Briggs, R.J. Nicholas, Nature Materials 4 (2005) 481.

12. Y. K. Chen, A. Chu, J. Cook, M. L. H. Green, P. J. F. Harris, R. Heesom, M. Humphries, J. Sloan, S.C. Tsang, J. F. C. Turner, Journal of Materials Chemistry 7 (1997) 545.

13. J. Sloan, M.C. Novotny, S.R. Bailey, G. Brown, C. Xu, V.C. Williams, S. Friedrichs, E. Flahaut, R.L. Callender, A.P.E. York, K.S. Coleman, M.L.H. Green, R.E. Dunin-Borkowski, J.L. Hutchison, Chemical Physics Letters 329 (2000) 61.

14. R. Carter, J. Sloan, A. I. Kirkland, R. R. Meyer, P. J. D. Lindan, G. Lin, M. L. H. Green, A. Vlandas, J. L. Hutchison, J. Harding, Phys. Rev. Lett., 96 (2006) pp215501/1-4.

15. N.A. Kieselev, A.S. Kumskov, V.G. Zhigalina, A.L. Vasiliev, J. Sloan, N.S. Falaleev, N.I. Verbitskiy, A.A. Eliseev, Journal of Microscopy 262 (2016) 92.

16. D.G. Calatayud, H. Ge, N. Kuganathan, V. Mirabello, R.M.J. Jacobs, N.H. Rees, C.T. Stoppiello, A.N. Khlobystov, R.M. Tyrrell, E.D. Como, S.I. Pascu, ChemistryOpen 7 (2018) 144.

17. A.A. Eliseev, N.S. Falaleev, N.I. Verbitskiy, A.A. Volykhov, L.V. Yashina, A.S. Kumskov, V.G. Zhigalina, A.L. Vasiliev, A.V. Lukashin, J. Sloan, N.A. Kiselev, Nano Letters 17 (2017) 805.

18. L. A. De Souza, C. A. S. Nogueira, J. F. Lopes, H. F. Dos Santos and W. B. De Almeida, Journal of Inorganic Biochemistry, 2013, 129, 71-83.

19. L. A. De Souza, C. A. S. Nogueira, P. F. R. Ortega, J. F. Lopes, H. D. R. Calado, R. L. Lavall, G. G. Silva, H. F. Dos Santos and W. B. De Almeida, Inorganica Chimica Acta, 2016, 447, 38-44.

20. L. A. D. Souza, C. A. S. Nogueira, J. F. Lopes, H. F. D. Santos and W. B. D. Almeida, The Journal of Physical Chemistry C, 2015, 119, 8394-8401.

21. E. Bichoutskaia, Z. Liu, N. Kuganathan, E. Faulques, K. Suenaga, I. J. Shannon and J. Sloan, Nanoscale, 2012, 4, 1190-1199.

22. J. Sloan, E. Bichoutskaia, Z. Liu, N. Kuganathan, E. Faulques, K. Suenaga and I. J. Shannon, Journal of Physics: Conference Series, 2012, 371, 012018.

23. T. Zoberbier, T. W. Chamberlain, J. Biskupek, N. Kuganathan, S. Eyhusen, E. Bichoutskaia, U. Kaiser and A. N. Khlobystov, Journal of the American Chemical Society, 2012, 134, 3073-3079.

24. A. Chuvilin, E. Bichoutskaia, M. C. Gimenez-Lopez, T. W. Chamberlain, G. A. Rance, N. Kuganathan, J. Biskupek, U. Kaiser and A. N. Khlobystov, Nature Materials, 2011, 10, 687.

25. Z. Hu, G. D. Pantoş, N. Kuganathan, R. L. Arrowsmith, R. M. J. Jacobs, G. Kociok-Köhn, J. O'Byrne, K. Jurkschat, P. Burgos, R. M. Tyrrell, S. W. Botchway, J. K. M. Sanders and S. I. Pascu, Advanced Functional Materials, 2012, 22, 503-518.

26. S. I. Pascu, N. Kuganathan, L. H. Tong, R. M. J. Jacobs, P. J. Barnard, B. T. Chu, Y. Huh, G. Tobias, C. G. Salzmann, J. K. M. Sanders, M. L. H. Green and J. C. Green, Journal of Materials Chemistry, 2008, 18, 2781-2788.

27. B. Mao, D. G. Calatayud, V. Mirabello, N. Kuganathan, H. Ge, R. M. J. Jacobs, A. M. Shepherd, J. A. Ribeiro Martins, J. Bernardino De La Serna, B. J. Hodges, S. W. Botchway and S. I. Pascu, Chemistry – A European Journal, 2017, 23, 9772-9789.

28. J. Lu, S. Nagase, X. Zhang, D. Wang, M. Ni, Y. Maeda, T. Wakahara, T. Nakahodo, T. Tsuchiya, T. Akasaka, Z. Gao, D. Yu, H. Ye, W. N. Mei and Y. Zhou, Journal of the American Chemical Society, 2006, 128, 5114-5118.

29. E.L. Sceats.; J. C. Green.; S. Reich, Phys Rev B 73 (2006) 125441.

30. N. Kuganathan, J.C. Green, International Journal of Quantum Chemistry 108 (2008) 797.

31. N. Kuganathan, J.C. Green, Chemical Communications (2008) 2432.

32. N. Kuganathan, J.C. Green, International Journal of Quantum Chemistry 109 (2009) 171.

33. N. Kuganathan, E-Journal of Chemistry 6 (2009).

34. R. Carter, M. Suyetin, S. Lister, M.A. Dyson, H. Trewhitt, S. Goel, Z. Liu, K. Suenaga, C.

Giusca, R.J. Kashtiban, J.L. Hutchison, J.C. Dore, G.R. Bell, E. Bichoutskaia, J. Sloan, Dalton Transactions 43 (2014) 7391.

35. I.Y. Gotlib, A.K. Ivanov-Schitz, I.V. Murin, A.V. Petrov, R.M. Zakalyukin, The Journal of Physical Chemistry C 116 (2012) 19554.

36. C. Fu, M. B. Oviedo, Y. Zhu, A. von Wald Cresce, K. Xu, G. Li, M. E. Itkis, R. C. Haddon, M. Chi, Y. Han, B. M. Wong and J. Guo, ACS Nano, 2018, 12, 9775-9784.

37. G. Li, C. Fu, M. B. Oviedo, M. Chen, X. Tian, E. Bekyarova, M. E. Itkis, B. M. Wong, J. Guo and R. C. Haddon, Journal of the American Chemical Society, 2016, 138, 40-43.

38. G. Kresse, & J. Furthmüller. Phys. Rev. B 54 (1996) 11169-11186.

39. G. Kresse, G & D. Joubert, Phys. Rev. B 59 (1999) 1758-1775.

40. J. P. Perdew, K. Burke, & M. Ernzerhof, Phys. Rev. Lett. 77 (1996) 3865-3868.

41. P. E. Blöchl, Physical Review B, 1994, 50, 17953-17979.

42. W. H. Press, S. A. Teukolsky,W. T. Vetterling, & B. P. Flannery, *Numerical recipes in C (2nd ed.): the art of scientific computing.* (Cambridge University Press, 1992).

43. H.J. Monkhorst, J.D. Pack, Physical Review B 13 (1976) 5188.

44. S. Grimme, J. Antony, S. Ehrlich, H. Krieg, The Journal of Chemical Physics 132 (2010) 154104.

45. N. Kuganathan, A. K. Arya, M. J. D. Rushton and R. W. Grimes, Carbon, 2018, 132, 477-485.

46. F.D. Murnaghan Proc. Natl. Acad. Sci. U. S. A., 30 (1944), p. 244.

47. S. Lalitha, S.Z. Karazhanov, P. Ravindran, S. Senthilarasu, R. Sathyamoorthy, J. Janabergenov, Physica B: Condensed Matter 387 (2007) 227.

48. J. Polit, E.M. Sheregii, J. Cebulski, B.V. Robouch, A. Marcelli, M.C. Guidi, M. Piccinini, A. Kisiel, P. Zajdel, E. Burattini, A. Mycielski, Journal of Applied Physics 100 (2006) 013521.

49. K. Strössner, S. Ves, W. Dieterich, W. Gebhardt, M. Cardona, Solid State Communications 56 (1985) 563.

50. T.F. Smith, G.K. White, Journal of Physics C: Solid State Physics 8 (1975) 2031.

51. S. Ouendadji, S. Ghemid, F E H MeradjiHand Hassan Comput. Mater. Sci. 50 (2011)1460.

52. S. Zerroug , F.A. Sahraoui and N. Bouarissa Eur. Phys. J. B 57 (2007) 9.

53. Y. Al-Douri, A. H. Reshak, H. Baaziz , Z. Charifi, R. Khenata, S. Ahmad and U. Hashim Sol. Energy 84 (2010) 1979.

54. C. Kittel, Introduction to Solid State Physics 6th edn (New York: John Wiley) p185, 1986.

55. W. H. Strehlow and E. L. Cook, Journal of Physical and Chemical Reference Data, 1973, 2, 163-200.

Table 1. Calculated and experimental lattice constants and bulk modulus of CdTe zinc blende structure.

Parameter	This study	Experiment	Other calculation
Lattice constant, a /Å	6.54	6.53[47], 6.49[48]	6.62-6.68[51-53]
Bulk modulus, B_0/GPa	39.1	42[49], 45[50]	33.8[51], 39.0[52], 36.6[53]

Table 2. Relative energy per CdTe unit of three 1-d CdTe motifs

Starting structure	Relative energy (eV/CdTe)
2:2	0.82
3:3	0.07
4:4	0.46
4:2	0.00

Table 3. Bond lengths, bond angles, encapsulation energies and charge transfer calculated for **4:2** CdTe crystals encapsulated within SWNTs.

Composites	d_t /Å	Cd-Te/Å	Cd-Te-Cd (°)	Te-Cd-Te (°)	E_{encap}/eV	Charge Transfer ($|e|$)
4:2@(8,8)	10.85	2.67-2.69	86.7-106.8	116.4-120.1	+0.47	−0.43
4:2@(9,9)	12.36	2.77-2.79	84.1-101.5	115.8-125.9	−0.33	−0.21
4:2@(10,10)	13.56	2.82, 2.83	82.1-99.6	114.8-128.6	−0.38	−0.12
1-d CdTe	−	2.81-2.83	81.2-99.1	114.1-128.8	−	−

Table 4. Bond lengths, bond angles, encapsulation energies and charge transfer calculated for **3:3** CdTe crystals encapsulated within SWNTs.

Composites	Cd-Te/Å	Cd-Te-Cd (°)	Te-Cd-Te (°)	E_{encap}/eV	Charge Transfer ($|e|$)
3:3@(9,9)	2.68-2.72	89.2-89.5	105.1-127.9	−0.12	−0.59
3:3@(10,10)	2.75-2.78	89.3-90.3	101.9-129.4	−0.30	−0.43
1-d CdTe	2.77-2.80	88.8	106.2-126.9	—	—

Table 5. Bond lengths, bond angles, encapsulation energies and charge transfer calculated for **4:4** CdTe crystals encapsulated within SWNTs.

Composites	Cd-Te/Å	Cd-Te-Cd (°)	Te-Cd-Te (°)	E_{encap}/eV	Charge Transfer ($|e|$)
4:4@(8,8)	2.87-2.92	76.6, 82.7, 161.2	95.8, 103.4, 161.3	−0.34	−0.48
4:4@(9,9)	2.93-2.96	70.9, 79.0, 153.0	97.9, 109.1, 153.0	−0.45	−0.35
4:4@(10,10)	2.95-2.98	69.5. 78.3, 151.2	98.2, 110.4, 151.1	−0.31	−0.19
1-d CdTe	2.92-3.00	69.9, 78.6, 152.2	97.9, 110.1, 152.2	–	–

Table 6. Bond lengths, bond angles, encapsulation energies and charge transfer calculated for **2:2** CdTe crystals encapsulated within SWNTs.

Composites	Cd-Te/Å	Cd-Te-Cd (°)	Te-Cd-Te (°)	E_{encap}/eV	Charge Transfer ($|e|$)
2:2@(8,8)	2.60, 2.61	91.6	173.0	−0.94	−0.13
2:2@(9,9)	2.66, 2.67	90.3	176.9	−1.07	−0.09
2:2@(10,10)	2.68	89.8	176.5	−0.84	−0.05
1-d CdTe	2.67	89.7	176.9	−	−
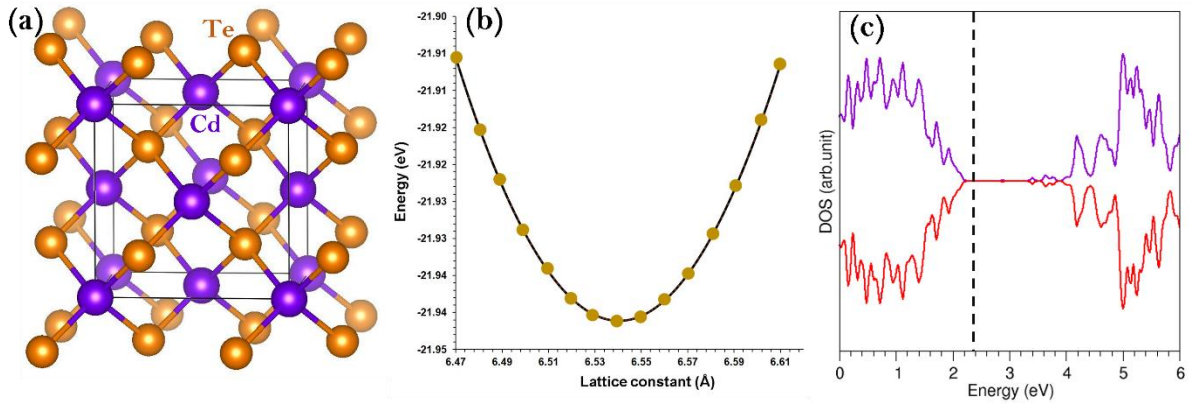
Figure 1. (a) Crystal structure of zinc blende CdTe, (b) plot of total energy versus lattice constant (brown circles are the points obtained by calculations, the line represents the Murnaghan fit) and (c) DOS plot calculated for bulk CdTe.
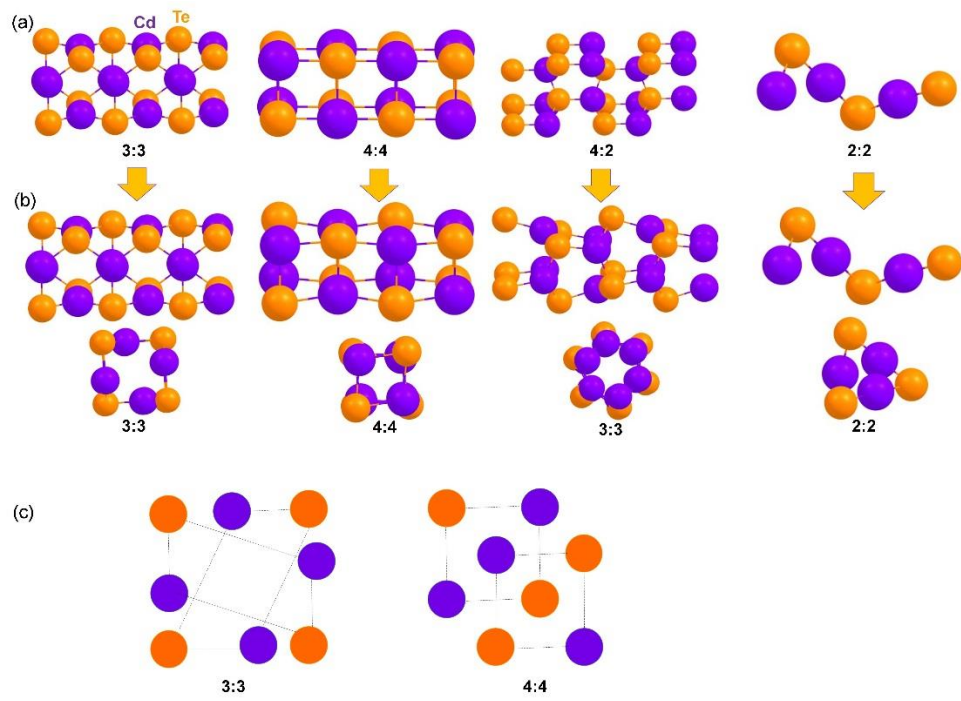
Figure 2. (a) Four different starting structures of one dimensional CdTe (b) corresponding optimised structures and (c) initial **3:3** and **4:4** structures showing a parallelogram and a square respectively.
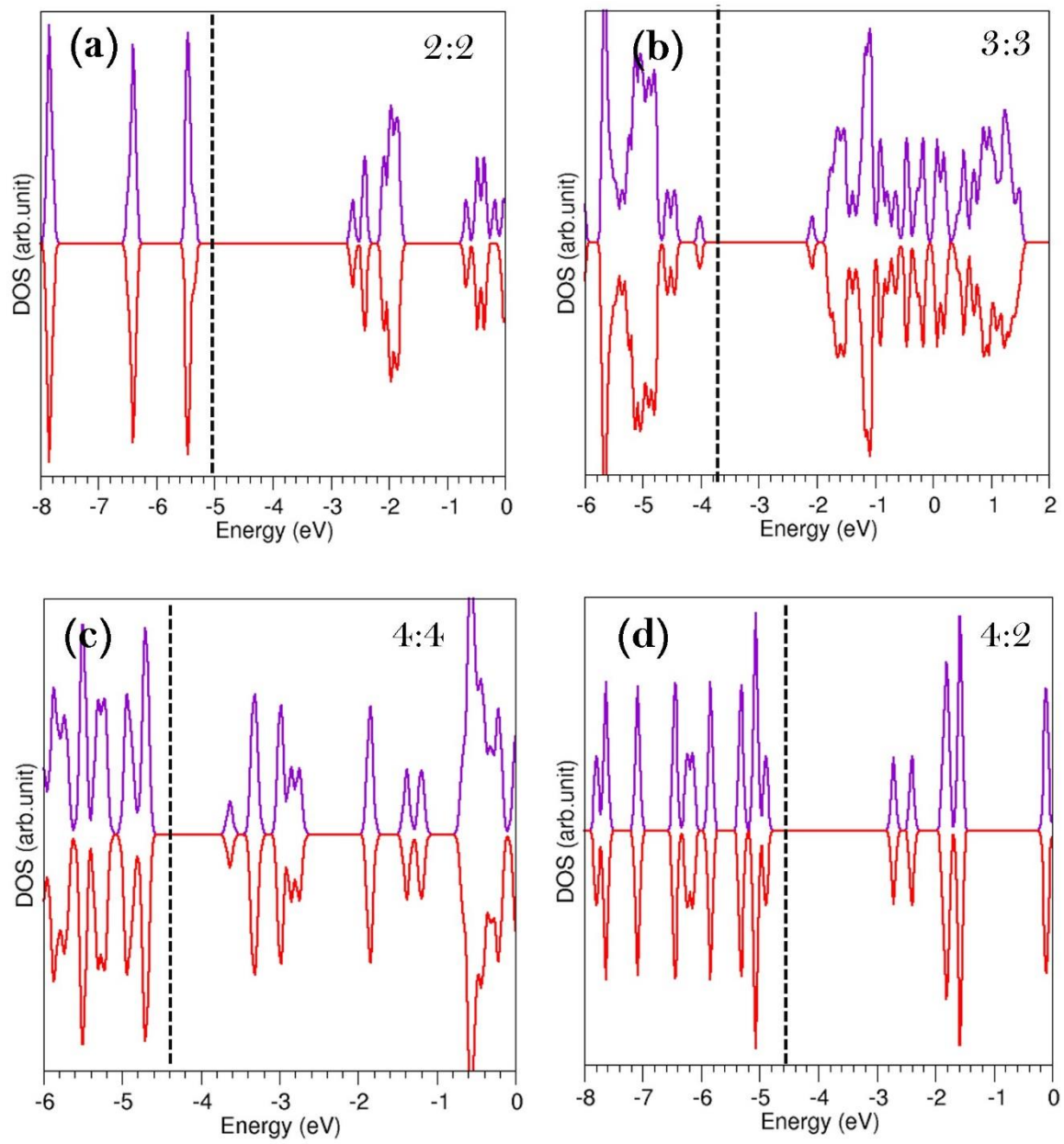
Figure 3. Densities of states of gas-phase one dimensional CdTe structures: (a) **2:2**, (b) **3:3**, (c) **4:4** and (d) **4:2**. Black dot-lines correspond to the Fermi energy level.
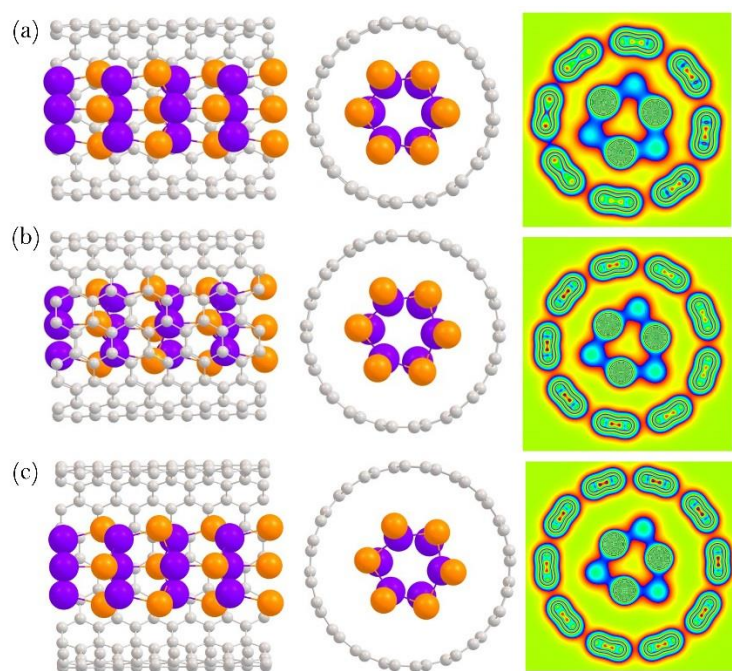
Figure 4. Optimised geometries and charge density plots for the **4:2** CdTe nanocrystals encapsulated within (a) (8,8) (b) (9,9) and (c) (10,10) SWNTs.
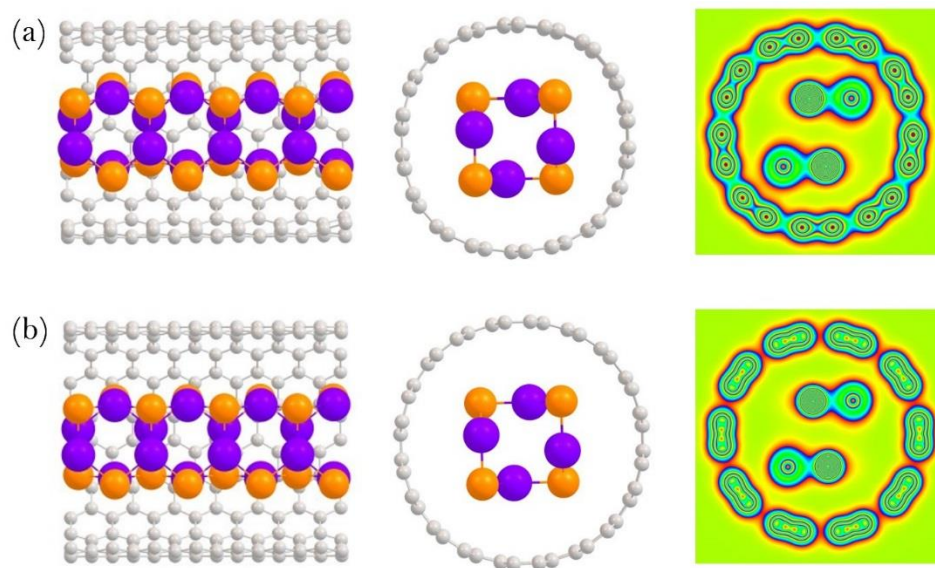
Figure 5. Optimised geometries and charge density plots for the **3:3** CdTe nanocrystals encapsulated within (a) (9,9) and (b) (10,10) SWNTs.
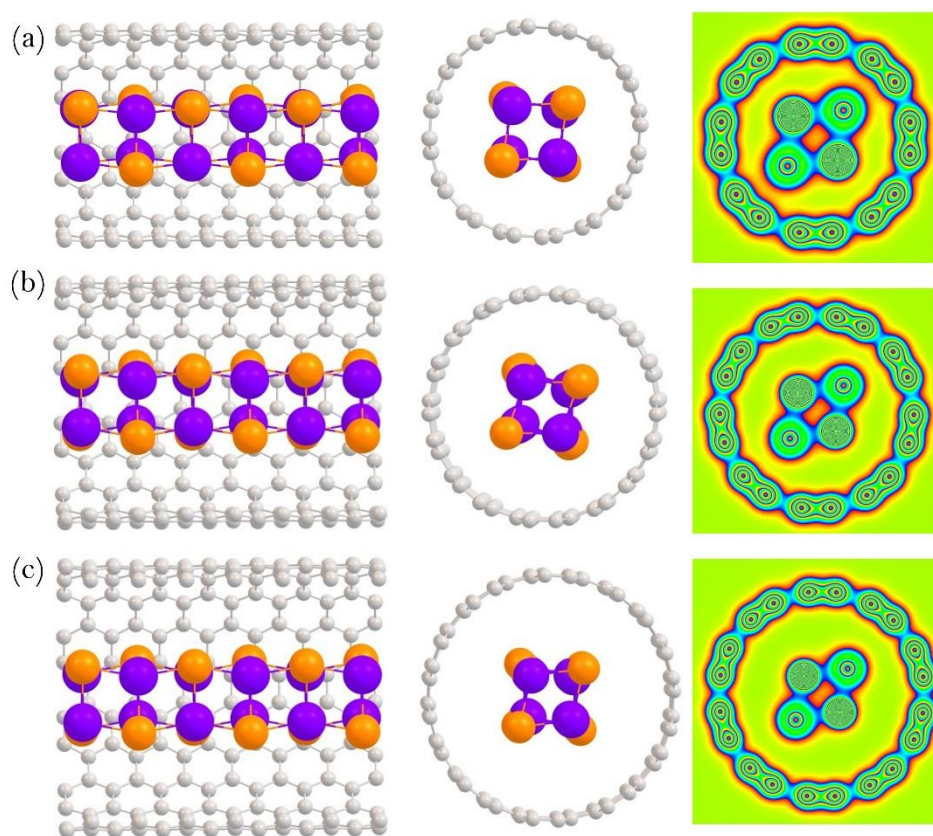
Figure 6. Optimised geometries and charge density plots for the **4:4** CdTe nanocrystals encapsulated within (a) (8,8) (b) (9,9) and (c) (10,10) SWNTs.
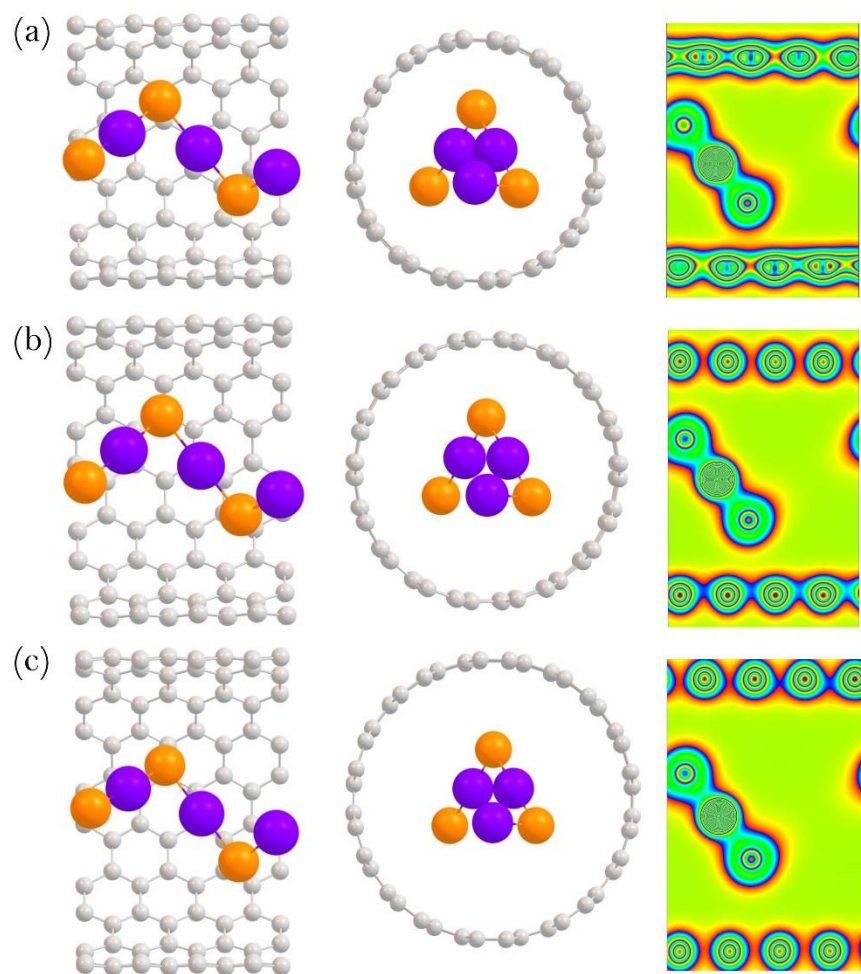
Figure 7. Optimised geometries and charge density plots for the **2:2** CdTe nanocrystals encapsulated within (a) (8,8) (b) (9,9) and (c) (10,10) SWNTs.